Vol. 35 No. 8 SCIENCE IN CHINA (Series A) August 1992

DOMAIN DECOMPOSITION HYBRID METHOD FOR NUMERICAL SIMULATION OF BLUFF BODY FLOWS*

——THEORETICAL MODEL AND APPLICATION

LING GUO-CAN (凌国灿)
(*Institute of Mechanics, Academia Sinica, Beijing* 100080, *PRC*)

LING GUO-PING (凌国平)
(*Department of Mechanics, Huazhong University of Science and Technology, Wuhan* 430074, *PRC*)

AND WANG YUN-PING (王运平)
(*Institute of Mechanics, Academia Sinica, Beijing* 100080, *PRC*)

Received July 6, 1991.

ABSTRACT

The discrete vortex method is not capable of precisely predicting the bluff body flow separation and the fine structure of flow field in the vicinity of the body surface. In order to make a theoretical improvement over the method and to reduce the difficulty in finite-difference solution of N-S equations at high Reynolds number, in the present paper, we suggest a new numerical simulation model and a theoretical method for domain decomposition hybrid combination of finite-difference method and vortex method. Specifically, the full flow field is decomposed into two domains. In the region of $O(R)$ near the body surface (R is the characteristic dimension of body), we use the finite-difference method to solve the N-S equations and in the exterior domain, we take the Lagrange-Euler vortex method. The connection and coupling conditions for flow in the two domains are established. The specific numerical scheme of this theoretical model is given. As a preliminary application, some numerical simulations for flows at $Re=100$ and $Re=1000$ about a circular cylinder are made, and compared with the finite-difference solution of N-S equations for full flow field and experimental results, and the stability of the solution against the change of the interface between the two domains is examined. The results show that the method of the present paper has the advantage of finite-difference solution for N-S equations in precisely predicting the fine structure of flow field, as well as the advantage of vortex method in efficiently computing the global characteristics of the separated flow. It saves computer time and reduces the amount of computation, as compared with pure N-S equation solution. The present method can be used for numerical simulation of bluff body flow at high Reynolds number and would exhibit even greater merit in that case.

Keywords: domain decomposition, hybrid method, finite-difference method, vortex method, numerical simulation, circular cylinder-separated flow.

* Project supported by the National Natural Science Foundation of China and the Lab for Nonlinear Mechanics, Institute of Mechnics, Academia Sinica.

I- Introduction

The vortex method (VM) and the finite difference method for N-S equations (FDM) are the two major methods for numerical simulation of bluff body flows. The advantages of the vortex method include what follows: It is capable of predicting effectively the global features of unsteady separated flow and the flow field far from the vorticity layer. Because this method is discrete only with respect to vorticity sheets, but not with respect to the whole velocity field, it is relatively time-saving in computation. The Lagrangian vortex method can avoid troubles brought about by grid dividing. With VIC method the amount of computation can be reduced from $O(N^2)$ (N is the number of vortex points) to the order of $O(M\log_2 M)$ (M is the number of grid nodes). The random walk can reflect the diffusion of vorticity. But the vortex method has a few intrinsic theoretical defects, for example, it is not capable of precisely predicting the flow field near the body surface and that near the vorticity layer. Prediction of the flow separation and vorticity distribution on the surface requires smoothing technique for computed results, providing approximate values in an average sense. The precision of the method with superposed random walk is proportional to $1/\sqrt{N}$. Consequently, to ensure the sufficient precision, the order of vortex number must be $O(Re)$, thus requiring a large amount of computation. In practice, the degree of precision is not satisfactory. In addition, essentially, the random walk of vortex can only simulate the viscous diffusion of fluid molecules. At high Reynolds number, the flow becomes turbulence, the definite meaning of this diffusion would be lost. Although a lot of results given by this method are rather satisfactory, its mechanism is still somewhat questionable. Using any kind of vortex method, a number of somewhat arbitrary parameters must be introduced in order to bring the numerical results into agreement with experimental data. On the other hand, in the case of moderate Reynolds number, the finite difference solution of N-S equations can yield very precise results of numerical simulation. But when the Reynolds number increases, the number of grid nodes should reach $O(Re)$, and the small scale structure with magnitude of $O(\sqrt{\nu})$ in the flow, e.g. the important deformation character of the flow, such as flow separation, secondary separation, would then be resolved precisely. This is difficult to realize at very high Reynolds number (e. g. $Re\sim 10^5$, 10^6, in the range of flow transition, or in the case of even higher Reynolds number). In addition, it needs even greater number of grid nodes and larger amount of computation to make the far wake flow field discrete. In the simulation of unsteady flow and vortex shedding, considerable amount of computation is required and different time steps are introduced to show the difference in character between starting flow and that of long-time flow. Moreover, there are still some theoretical problems in finite-difference solution for flow at high Reynolds number remaining to be solved.

Considering both the advantages and the existing problems of the two methods mentioned above, we try in the present work to explore a new kind of numerical model, expecting that it not only is capable of giving precise description of fine structure of flow near body surface, and the generation and initial convection of vorticity, but also can conveniently yield precise computed results for a large scale

flow and predict the overall characteristics of the flow far from the body surface. For this purpose, in the persent paper, we suggest and study a domain decomposition hybrid combination method for finite-difference solution of N-S equations and a vortex method. This method possesses the advantages of finite-difference solution of N-S equations. It will reduce the difficulty of large number of grid nodes and large amount of computation for high resolution required by treating flow at high Reynolds number by means of limiting the region to be studied in detail to the area near the bluff body. At the same time, this method also has the advantages of discrete vortex method and can be used to predict the character of flow in region with large extent. In order to make full use of some previous results for detailed comparisons, in the present paper the new method will be applied to simulating flows at moderate Reynolds number around a circular cylinder, and the computed results of $Re = 100$ and $Re = 1000$ will be given. For the purpose of analysis and comparison, the corresponding finite-difference solution of N-S equations for full flow field will also be computed, and the influence of location of interface between the two domains is estimated. In the following paper, we will present the results for high Reynolds number and unsteady flow cases by the new method with a high order difference scheme used.

II. Theoretical Method

1. *Domain Decomposition and Fluid Flow Resolution by Hybrid FDM-VM Method*

The complete flow field is decomposed into two domains, namely, the interior domain Ω_1 and the exterior domain Ω_2. The interface between Ω_1 and Ω_2 is I, as shown in Fig. 1.

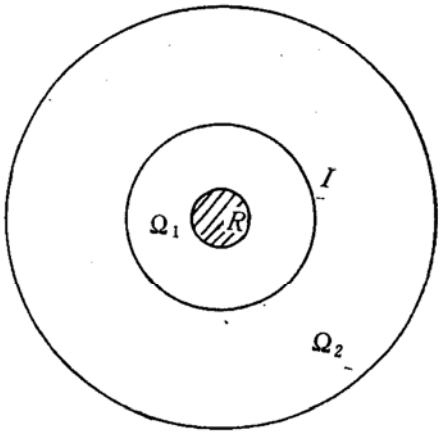

Fig. 1.

The interior flow is viscous, flow separation occurs and important deformation exists there. This is the region where the vorticity takes place and transports initially, The extent of this region is $O(\sqrt{\nu})$. But in view of the fact that the complex structure of flow in reverse flow region should be shown and that the reduction of the circulation of vortices in near wake would significantly influence the force acting on the body, the extent of interior domain can be extended to $O(R)$(R is a characteristic dimension of the body). This range can be determined flexibly according to our requirement on precision of describing the fine structure of flow and the requirement on amount of computation. In domain Ω_1 the variation of vorticity and the flow field are determined by N-S equations and Poisson equation about stream function and their initial and boundary conditions for this solution. The boundary values of vorticity on the interface must be determined with care. The flow in domain Ω_2 is assumed approximately to be inviscid potential flow. The convection of vortex is calculated using discrete vortex model and VIC method[1]. The

vorticity is conserved when the vortex is in motion. The velocity of this motion is given by Poisson equation.

The flows in the two domains are coupled together, and will be solved simultaneously. The exterior domain gains the newly generated discrete vortex from vorticity flux passing across the interface, which serves as the initial condition for solving the vortex motion in the exterior domain. The vortex motion in the exterior domain is determined by using the full flow field vorticity distribution and by solving the Poisson equation. In solving the interior N-S equations, the boundary condition ω_I at the interface is given by interpolation for the vorticity on the two sides near the interface, i.e.

$$\omega_I(i,j) = \sum_{k=I-1}^{I+N} \Delta\omega_k, \tag{1}$$

where $\Delta\omega_k$ is the discrete vortex component on the interface, such discrete vortices were generated from the vorticity at grid nodes of the k-th grid layer, and experienced a motion for one time step. N is a positive integer. The stream function values ψ_I on the interface are obtained from interpolation of nearby stream function determined by the vorticity of the full flow field. Across the domain interface the mass flux, the momentum flux and the vorticity flux should be conserved. The correlation and simultaneous solution of flows in Ω_1 and Ω_2 can also be visualized from the computation methods presented in the next section.

2. *Interior-Exterior Domain Hybrid Computation Method*

The interior domain and the full flow field are divided with fine and coarse grids respectively. Two sets of grid, fine and coarse, can be applied simultaneously to the interior domain. The computation method is as follows.

(1) As the variables on the interface at the n-th time step are known, solve the N-S equations on the fine grid in Ω_1. Then vorticity distribution is obtained.

(2) Calculate the new discrete vortex transferring into Ω_2 and the movement of discrete vortex originally existing in Ω_2. Vorticity in Ω_2 is obtained.

(3) Solve the Poisson equation from full field vorticity distribution. The stream function and the velocity on the coarse grid are obtained.

(4) Calculate the vorticity, the stream function and the velocity on the interface required by the next time step.

(5) Solve the Poisson equation on fine grid in Ω_1 to obtain values of stream function, and calculate the velocity field and the vorticity on the body surface, as well as the forces on the body.

Repeat steps (1)—(5) to obtain the flow solution.

3. *Method of Numerical Solution*

(1) *The governning equations and the determining conditions*

Let flow variables, time variable and coordinate variables ω, Ψ, V_r, V_θ, t and r

be made dimensionless by introducing characteristic quantities $\frac{U_\infty}{R}$, $U_\infty R$, U_∞, $\frac{R}{U_\infty}$ and R. In order to make the grid denser in the vicinity of cylinder surface, we introduce the following coordinate transformation:

$$r = \exp(2\pi\xi),$$
$$\theta = 2\pi\eta \tag{2}$$

to transform the physical plane (r, θ) of the rounded flow into the computational plane (ξ, η).

For the interior domain, the governning equations of the flow around a circular cylinder and the solution-determining conditions are as follows:

$$D.E_s. \qquad E\frac{\partial\omega}{\partial t} + \frac{\partial}{\partial\xi}(U\omega) + \frac{\partial}{\partial\eta}(V\omega) = \frac{2}{Re}\left(\frac{\partial^2\omega}{\partial\xi^2} + \frac{\partial^2\omega}{\partial\eta^2}\right), \tag{3a}$$

$$\frac{\partial^2\psi}{\partial\xi^2} + \frac{\partial^2\psi}{\partial\eta^2} = -E\omega,$$

where $E = 4\pi^2\exp(4\pi\xi)$, $U = \frac{\partial\psi}{\partial\eta} = E^{\frac{1}{2}}V_r$, $V = -\frac{\partial\psi}{\partial\xi} = E^{\frac{1}{2}}V_\theta$ (V_r, V_θ present the velocity components in physical plane).

$$B.C. \qquad \xi = 0 \quad \psi = \frac{\partial\psi}{\partial r} = 0, \quad \omega = -\frac{1}{E}\frac{\partial^2\psi}{\partial\xi^2},$$

$$\xi = \xi_I \ \omega_I(\xi,\eta) \text{ to be given},$$
$$\psi_I(\xi,\eta) \text{ to be given}, \tag{3b}$$

$$I.C. \qquad t = 0 \quad \psi = -2\mathrm{sh}(2\pi\xi)\sin(2\pi\eta),$$
$$\omega(\xi,\eta) = 0. \tag{3c}$$

The dimensionless pressure P, and shear stress $\left(\text{normalized by}\frac{1}{2}\rho V_\infty^2\right)$ τ_w and the vorticity ω on the cylinder surface can be obtained from the following relations:

$$\left.\frac{\partial p}{\partial\eta}\right|_{\xi=0} = \frac{4}{Re}\left.\frac{\partial\omega}{\partial\xi}\right|_{\xi=0}, \tag{4}$$

$$\tau_\omega = f(\eta) = \frac{4}{Re}\left.\omega\right|_{\xi=0}, \tag{5}$$

$$\omega_{\xi=0} = -\left(\frac{1}{E}\frac{\partial^2\psi}{\partial\xi^2}\right)_{\xi=0}. \tag{6}$$

The coefficients of drag and transverse force with $\frac{1}{2}\rho U_\infty^2$ as a reference quantity are

$$-C_D + iC_L = \frac{2}{R_e}\, i\int_0^1\left(2\pi\omega - \frac{\partial\omega}{\partial\xi}\right)_{\xi=0} e^{i2\pi\eta}d\eta. \tag{7}$$

(2) *The finite difference equations*

For flow at moderate Reynolds number, in the present paper, the revised expo-

nential type finite-difference scheme derived by Kellogg[2] is utilized to treat two-dimensional unsteady flow, and the alternation direction implicit (ADI) method is employed to perform alternating direction implicit difference calculation in directions ξ and η, then the finite-difference equations for N-S equations are obtained as follows:

$$E_i \frac{\tilde{\omega}_{i,j} - \omega^n_{i,j}}{\frac{\Delta t}{2}} + \frac{(U\omega)^n_{i+1,j} - (U\omega)^n_{i-1,j}}{2\Delta\xi} + \frac{(V^n\tilde{\omega})_{i,j+1} - (V^n\tilde{\omega})_{i,j-1}}{2\Delta\eta}$$

$$= \frac{2}{Re}\left[\frac{(\sigma_1\omega)^n_{i+1,j} - 2(\sigma_1\omega)^n_{i,j} + (\sigma_1\omega)^n_{i-1,j}}{\Delta\xi^2}\right.$$

$$\left. + \frac{(\sigma^n_2\tilde{\omega})_{i,j+1} - 2(\sigma^n_2\tilde{\omega})_{i,j} + (\sigma^n_2\tilde{\omega})_{i,j-1}}{\Delta\eta^2}\right], \tag{8a}$$

$$E_i \frac{\omega^{n+1}_{i,j} - \tilde{\omega}_{i,j}}{\frac{\Delta t}{2}} + \frac{(\tilde{U}\omega^{n+1})_{i+1,j} - (\tilde{U}\omega^{n+1})_{i-1,j}}{2\Delta\xi} + \frac{(\tilde{V}\tilde{\omega})_{i,j+1} - (\tilde{V}\tilde{\omega})_{i,j-1}}{2\Delta\eta}$$

$$= \frac{2}{Re}\left[\frac{(\tilde{\sigma}_1\omega^{n+1})_{i+1,j} - 2(\tilde{\sigma}_1\omega^{n+1})_{i,j} + (\tilde{\sigma}_1\omega^{n+1})_{i-1,j}}{\Delta\xi^2}\right.$$

$$\left. + \frac{(\tilde{\sigma}_2\tilde{\omega})_{i,j+1} - 2(\tilde{\sigma}_2\tilde{\omega})_{i,j} + (\tilde{\sigma}_2\tilde{\omega})_{i,j-1}}{\Delta\eta^2}\right], \tag{8b}$$

where

$$(\sigma_k)_{i,j} = \frac{(U_k)_{ij}\Delta l_k}{4} Re \coth\left[\frac{(U_k)_{ij}\Delta l_k}{4} Re\right], \quad k = 1,2 \tag{8c}$$

when $k = 1$, $V_1 = U$, $\Delta l_1 = \Delta\xi$; $k = 2$, $U_2 = V$, $\Delta l_2 = \Delta\eta$.

The symbol "$\sim$" implies taking the values at $\left(n + \frac{1}{2}\right)$-th time step. The Poisson equation in (3a) is solved by means of the successive over-relaxation (SOR) method, with the following scheme

$$\psi^{k+1}_{i,j} = \psi^k_{i,j} + \frac{\alpha}{2(1+\beta^2)}[\psi^k_{i+1,j} + \psi^{k+1}_{i-1,j} + \beta^2(\psi^k_{i,j+1} + \psi^{k+1}_{i,j-1})$$

$$+ (\Delta\xi)^2 E_i\omega_{i,j} - 2(1+\beta^2)\psi^k_{i,j}], \tag{9}$$

where $\beta = \Delta\xi/\Delta\eta$, α is the over-relaxation factor. Taking $\alpha = 1.72$, the rapid convergency can be affected.

One of the reasons why we adopt the above-mentioned difference scheme is that the program of ours for solving N-S equations may be used directly. Generally speaking, for the revised exponential finite-difference scheme of Kellogg, the precision is of the first-second order, the stability is good, the amount of computation is not large, the convergence speed is rapid, and the grid Reynolds number is not limited, so this scheme is appropriate for treating flow at low and moderate Reynolds numbers[3]. And the ADI method is capable of reducing the inversion of a 5-rank diagonal matrix into successive inversions of 3-rank matrices. This can save computer time greatly.

The surface vorticity and the vorticity gradient are calculated by using the

(3) *Lagrange/Euler vortex method calculation in exterior domain*

The strength of j-th nascent discrete vortex which is converted from the vorticity flux passing through the j-th section surface element $d\eta$ on the interface in unit time may be approximately expressed as

$$\Delta\Gamma_j = \int_j \omega_l U_n d\eta = \frac{1}{4}(\omega_j + \omega_{j+1})(U_{nj} + U_{nj+1})\Delta\eta\Delta t. \tag{12}$$

Here U_n is the normal velocity at the interface.

Assuming that vorticity flows out from the center of every small arc element on the interface with average velocities $U = \frac{1}{2}(U_j + U_{j+1})$, $V = \frac{1}{2}(V_j + V_{j+1})$, after Δt, each nascent discrete vortex will be located at

$$\begin{aligned} \xi(t + \Delta t) &= \xi(t, i) + \delta\xi, \\ \eta(t + \Delta t) &= \eta\left(t, j + \frac{1}{2}\right) + \delta\eta, \end{aligned} \tag{13a}$$

where

$$\begin{aligned} \delta\xi &= \frac{1}{2} U \cdot \Delta t/E, \\ \delta\eta &= \frac{1}{2} V \cdot \Delta t/E. \end{aligned} \tag{13b}$$

The movement of discrete vortex already in exterior domain can be calculated with VIC method. After Δt, each discrete vortex will be located at

$$\begin{cases} \xi(t + \Delta t) = \xi(t) + \delta\xi, \\ \eta(t + \Delta t) = \eta(t) + \delta\eta, \\ \delta\xi = U_p \cdot \Delta t/E, \\ \delta\eta = V_p \cdot \Delta t/E, \end{cases} \tag{14}$$

where U_p, V_p are velocities of vortex motion; they can be obtained from velocities on the grid nodes by using area-weighted interpolation method as follows:

$$\begin{aligned} U_p &= \sum_{k=1}^{4} u_k A_k / A, \\ V_p &= \sum_{k=1}^{4} v_k A_k / A, \end{aligned} \tag{15}$$

where u_k and v_k are flow field velocities on grid nodes, which can be derived from the solution of Poisson equation. A is the grid cell area and A_k is the area occupied by the k-th vortex. When the vortex with strength Γ reaches its new location, the corresponding vorticity distribution on grid nodes is

$$\omega_k = \frac{\Gamma}{E_k}\frac{A_k}{A^2}. \tag{16}$$

In the present computation, the spacing of the coarse grid is taken as integral multiple of that of fine grid in interior domain. In the calculation with discrete vortex method our previous study on the force prediction has shown that[4] the circulation reduction of vortex in the near wake ($1 < r < 3$) is expected to affect considerably the drag and transverse force, and the effect of vortex decay in the far field may be neglected, so that in our computation the interface between interior and exterior domains is taken to be located at $r = 2$—3.

III. Computation Results and Comparison

1. $Re = 100$

In the case of the $Re = 100$ solution, we take the same grid spacing in both interior and exterior domains on the computation plane, for comparison with the results of solution of full field N-S equations. Take $\Delta\xi = 0.01$, $\Delta\eta = 0.0167$. The interface between the two domains is a circular cylindrical surface of $r_I = 3$, i.e. being located on the grid points with $I = 18$, positioned at a radial distance 3 times the radius of the circular cylinder. The total number of grid nodes in the interior domain is $I \times J = 18 \times 60$, and the corresponding region on the physical plane is $1 \leqslant r \leqslant 3$, $0 \leqslant \theta \leqslant 2\pi$. The total number of grid nodes is $I \times J = 60 \times 60$, the corresponding region on physical plane is $1 \leqslant r \leqslant 43$, $0 \leqslant \theta \leqslant 2\pi$. The time step is $\Delta t = 0.02$. For the purpose of analysis and comparison, we make finite-difference solution of N-S equations for full flow field with the same numerical scheme and grid dividing. In addition, using the same method, we further calculate the flow in the early stage as the location of the interface is taken at $r_I = 2$, i.e. on the grid nodes with $I = 12$. Computation in the present paper gives the time variations of physical quantities, such as the drag of the circular cylinder, the transverse force, the separation point, the stagnation point, the surface pressure distribution, the vorticity distribution, the radial velocity on the symmetric axis behind the cylinder, the flow patterns, and the vortex shedding as well as S_t number.

The general features of the variations of these quantities coincide with those given by previous numerical solutions of N-S equations, which are omitted here. Table 1 gives the calculated global features of the separated flow and their comparison with available data. The results show that the mean value of the drag and S_t number are in excellent agreement with experimental results given by Relf et al.[5] and Roshko[6]. The mean value of separated angle agrees well with or is very close to the numerical solutions from Kawaguti[7], Jordan et al.[8] and Thoman et al.[9] The prediction of the global features of the flow given by the present method coincides well with that given by our finite-difference solutions of N-S equations

for full flow field.

Table 1

The Global Features of the Separated Flow About Circular Cylinder and the Comparison

Results	$\bar{C}_D$		$\bar{S}^0_\theta$		S_t		$C_{lr.m.s.}$
	$Re = 10^2$	10^3	10^2	10^3	10^2	10^3	10^2
Present method	1.435	1.17	116.6	96.4	0.163	0.203	0.229
FDM solution of NS eq. for full flow field by present work	1.41	1.15	115.9	96.2	0.16		
Experimental results	1.436 (Relf[5]) 1.60 (Wiselsberger[11])	1.00			0.16	0.213 (Roshko[6])	
Jordan et al.[8]	1.28	1.24	117	92	0.16	0.206	
Kawaguti[7]	1.20		115				
Thoman et al.[9]	1.50		117.5	102			

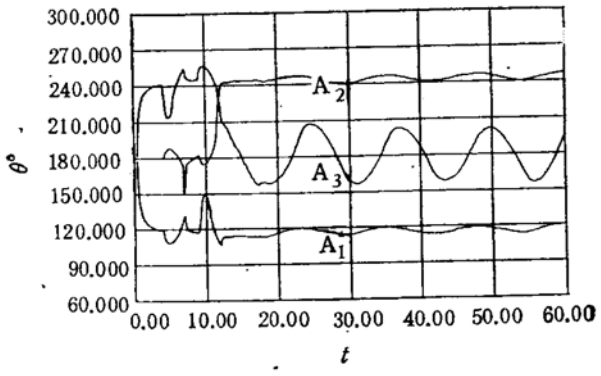

Fig. 2. Periodic variation of separation angles (A_1, A_2) and rear stagnation point ($Re = 100$).

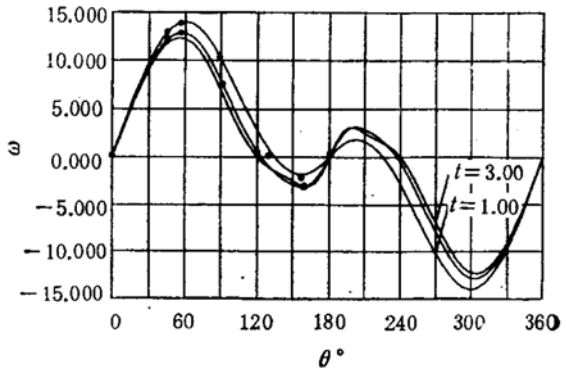

Fig. 3. Vorticity distribution at the cylinder surface and comparison between the present work and Ref. [10].
——, Present results; ···, Collins and Dennis'[10]

Fig. 2 shows the variations of the angle of separation and the rear stagnation point. The detailed change of the vorticity distribution with time and the separation at the cylinder surface are shown in Figs. 3 and 4 respectively. The comparison between our results and those given by Collins & Dennis[10] is made in the two figures and an excellent agreement is obtained.

Our computation shows that as $Re = 100$, the vorticity generated at the surface of the circular cylinder transports to domain interface, reaching there almost at $t = 1.36$. Hence, the coincidence shown in the comparison of vorticity at $t = 1.0$ and $t = 2.0$ in the figure demonstrates the correctness of our numerical solution of N-S equations for full flow field as the outer boundary shifts from infinity in theoretical sense to the finite region ($O(R)$) of $r_I = 3$, and the correctness

of the domain decomposition hybrid combination solution. Table 2 presents the detailed comparison of computed results of separation angle. It can be found from the table that for three cases in this paper, i.e. the domain decomposition hybrid combination solution, the full field N-S equations solution by the same numerical scheme, and the solution when the position of domain interface changes, the computed results are very close to each other. When the position of domain interface changes from $r_I = 3$ to $r_I = 2$, the present solution is stable. The computed values of drag in these three cases also show agreement. Figs. 5(a)—5(b) show the good periodicity for the stream line patterns at various instants, with a difference of about half a period. The

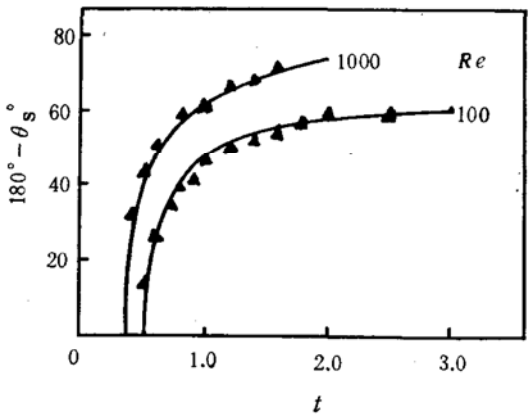

Fig. 4. Variation with time of the angle of separation
▲, Present results, ——, Collins and Dennis' numerical solutions.[10]

Table 2
Comparison of Angle of Separation ($Re = 100$)

t	Angle of Separation		
	Solution by present method		Finite-difference solution for N-S eq. for full flow field
	$r_I = 3$	$r_I = 2$	
0.5	166.90	166.75	166.88
1.0	133.32	133.53	134.13
1.5	126.35	126.33	126.84
2.0	123.41	123.42	123.31
2.5	121.57	122.00	121.68
3.0	120.07	120.34	120.07
3.5	119.33	119.45	119.39
4.0	118.59	118.86	118.61

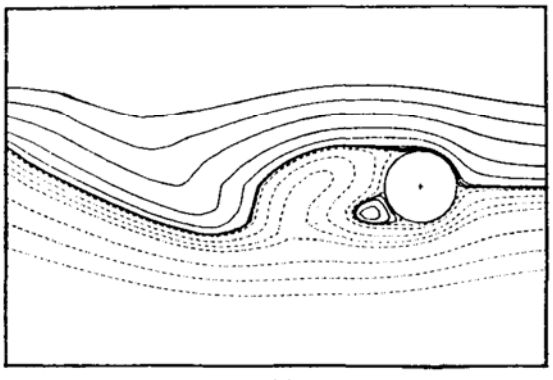

Fig. 5(a). Streamline pattern at $t = 52.0$ for $Re = 100$.

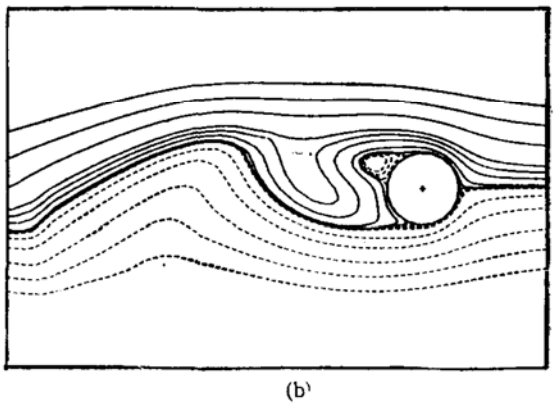

Fig. 5(b). Streamline pattern at $t = 58.0$ for $Re = 100$.

computation is done with a Honeywall DPS 8/52 computer. Up to $t = 60$, CPU time used is 1.2 h., while CPU time required by solving N-S equations for full flow field with the same finite-difference scheme is 1.9 h, the latter being 1.58 times of that required by the method suggested in the present paper.

2. $Re = 1000$

For $Re = 1000$, one computed example in this paper applies uniform grids in both interior and exterior domains on ξ, η plane and $\Delta\xi = 0.005$, $\Delta\eta = 0.0083$. The interface between the two domains is a circular cylinder with $r_i = 3$. The total number of grid nodes is $I \times J = 120 \times 120$. The corresponding flow region is $1 \leqslant r \leqslant 43$, $0 \leqslant \theta \leqslant 2\pi$. Time step is $\Delta t = 0.02$. The global features of the flow are given in Table 1. Comparison shows that the calculated drag coefficient is close to the measured values of Wieselsberger[11] and the numerical results of Jordan et al.[8]

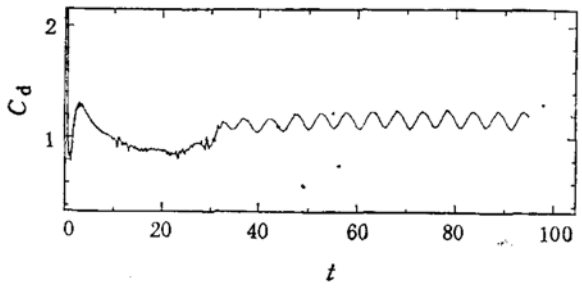

Fig. 6. Variation of drag coefficient with time ($Re = 1000$).

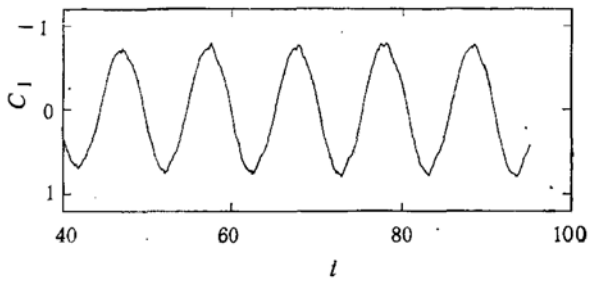

Fig. 7. Periodic variation of transverse force coefficient ($Re = 1000$).

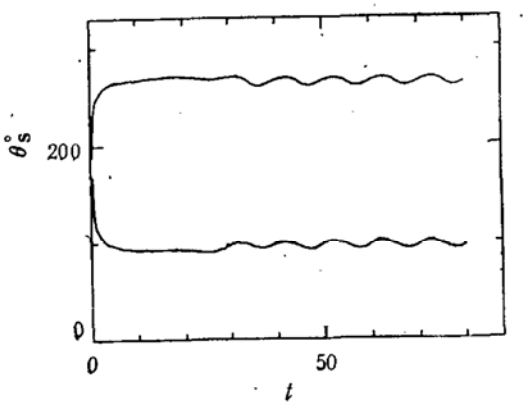

Fig. 8. Periodic variation of separation angles ($Re = 1000$).

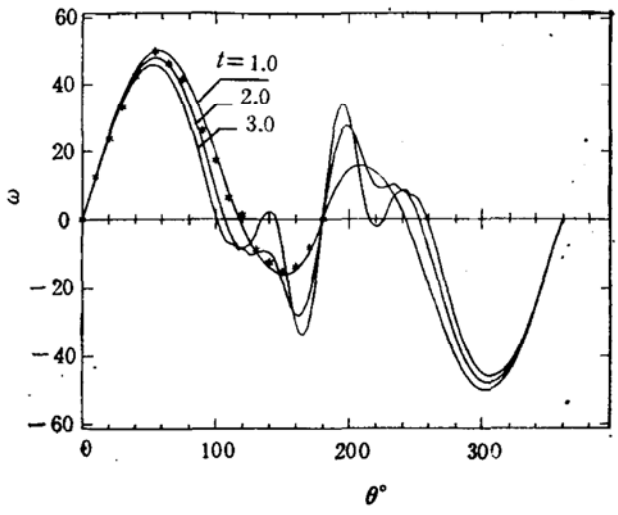

Fig. 9. Variation of vorticity distribution at the cylinder surface and comparisons between the present work and Ref. [10](Re=1000). ——, Present results; ***, Collins and Dennis' numerical solutions.

The calculation of S_t number agrees well with the results of Jordan et al.[8] It is close to the experimental data of Roshko[6] and is a bit lower. The prediction of the separation is close to the results of Jordan et al.[8], and more accurate than that given by Thoman et al.[9] The coincidence between the present results obtained by the domain decomposition hybrid method and numerical solution of N-S equations for full flow field is very good. Figs. 6—8 show the periodic variations of drag, transverse force and the separation point.

Table 3
Comparison of the Angles of Separation ($Re = 1000$)

t	Angle of Separation	
	Solution by present method	Finite-difference solution for N-S eq. for full flow field
1.0	117.74	117.67
1.2	114.74	114.68
1.4	112.47	112.13
1.6	110.29	110.17
1.8	108.61	108.45
2.0	106.95	106.79
2.2	105.46	105.31
2.4	104.15	104.50
2.6	102.91	102.84
2.8	101.67	101.79
3.0	100.89	101.01

The comparison of computed vorticity distribution on cylinder surface and the separation variation at the early stages of the flow with results of Collins and Dennis[10] are given in Figs. 9 and 4, respectively.

Both results coincide perfectly. The detailed comparison of calculated separation points for the early stage of the flow is presented in Table 3. It can be found that the coincidence of domain decomposition hybrid combination solution with that of N-S equations for full flow field using the same finite-difference scheme is even more perfect.

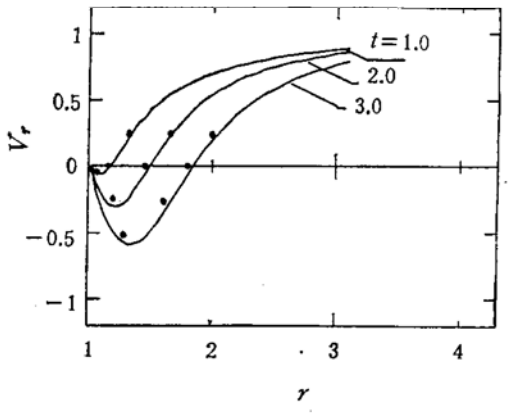

Fig. 10. Variation of the radial velocity on the symmetric axis behind the cylinder and comparisons between the present work and Ref. [12]($Re = 1000$). ——, Present results; ···, Ta Phuoc Loc's numerical solutions[12].

Fig. 10 shows the variation of radial velocity on symmetric axis behind the cylinder and their comparison with results by high order numerical schemes given by Ta Phuoc Loc[12]. It is found that the present method predicts accurately the velocity distribution. Shown in Figs. 11(a) and 11(b) are the computed results for stream line patterns at two instants with about one period interval which exhibit a perfect periodicity,

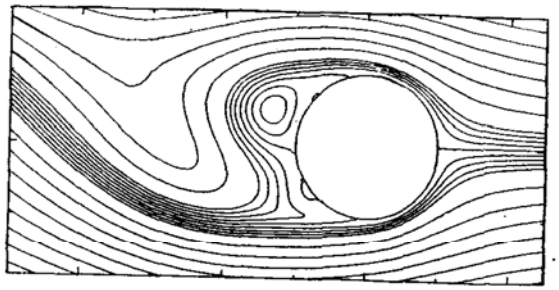

(a)

Fig. 11(a). Streamline pattern at $t = 82.0$ for $Re = 1000$.

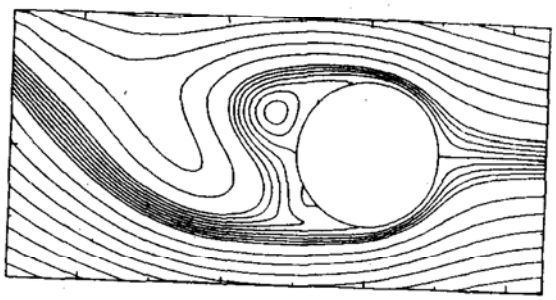

(b)

Fig. 11(b). Streamline pattern at $t = 92.0$ for $Re = 1000$.

revealing the kinematic features of the separated vortex flow.

In the present paper, computation of the flow is further carried out in another case. Fine grid is applied to the interior domain with $\Delta\xi = 0.0025$, $\Delta\eta = 0.0167$; and coarse grid is applied to both domains with $\Delta\xi = 0.01$, $\Delta\eta = 0.0167$. Interface of the two domains is taken at $r_I = 2$. Results very close to the available finite difference solution of N-S equations are also obtained. They will not be described in detail here, for space is limited. The computation is done with a Honey-wall DPS 8/52 computer. Up to $t = 4$, CPU time required by the domain decomposition hybrid solution is 2.1', while that required by solution of N-S equations for the full flow field with the same finite-difference scheme is 2.8', the latter being 1.33 times of that needed by the present method. Up to $t = 50$, CPU time required by the present method is 2 h.

IV. Conclusion

The present paper proposes a new numerical method of domain decomposition hybrid combination finite-difference of N-S equations and vortex method. Computation of circular cylinde-separated flows at moderate Reynolds numbers is presented. The numerical results on the separated flows at $Re = 100$ and 1000 show that our method is capable of satisfactorily predicting the flow characteristics in the vicinity of cylinder surface, such as flow separation, surface vorticity distribution and radial velocity variation, as well as the global flow features, such as periodic variations of the flow, drag, transverse force, vortex shedding and S_t number. The results of computation are in good agreement with or very close to the finite-difference solution of N-S equations for full flow field and experimental measurements. Our method also saves CPU time. Our theoretical model and numerical method, if further applied to treating flow at high Reynolds numbers and flow with complex unsteady oncoming, will show even greater advantages. Simulation of flow at high Reynolds number in the domain decomposition solution requires high order precision numerical scheme, such that details of small scale flow structure in the vicinity of cylinder surface can be obtained with satisfactory precision.

We thank Gu Qi-yang for his help in numerical calculations.

References

[1] Stansby, P. K. & Dixon, A. G., *Applied Ocean Research*, **5**(1983), 167.
[2] Kellogg, R. B. et al., *SIAM J. Numer. Anal.*, **17**(1980), 6: 733.
[3] Wang Ru-quan & Chen Bin, *J. Hydrodynamics* (in Chinese), **5**(1990), 4: 89.
[4] Ling Guo-can, *Acta Mechanica Sinica*, **4**(1988), 3: 211.
[5] Relf, F. F. & Simmons, L. F. G., *Aeronaut. Res. Coun. Rep. Mem.*, 1924.
[6] Roshko, A., *NACA TN* 2913, 1953.
[7] Kawaguti, J., *Phys. Soc. Japan*, **8**(1953), 747.
[8] Jordan, S. K. & Fromm, J. E., *The Physics of Fluids*, **15**(1972), 3.
[9] Thoman, D. C. & Szewczyk, A. A., *Physics of Fluid Supplement*, **12**(1969), 76.
[10] Collinis, W. M. & Dennis, S. C. R., *J. Fluid Mech.*, **60**(1973), part 1, 105.
[11] Wieselsberger, V. C., *Physik. Z.*, **22**(1921), 321.
[12] Ta Phuoc Loc, *J. Fluid Mech.*, **100**(1980), part 1, 111.